DALTON

Synthesis, platinum-195 nuclear magnetic resonance spectroscopic and extended X-ray absorption fine structure studies on platinum-(II) and -(IV) thioether macrocyclic complexes

Alexander J. Blake,[a,b] Melanie J. Bywater,[c] Rhona D. Crofts,[b] Alexander M. Gibson,[c] Gillian Reid *[,c] and Martin Schröder *[,a,b]

[a] *Department of Chemistry, The University of Nottingham, Nottingham NG7 2RD, UK*
[b] *Department of Chemistry, The University of Edinburgh, West Mains Road, Edinburgh EH9 3JJ, UK*
[c] *Department of Chemistry, The University of Southampton, Highfield, Southampton SO17 1BJ, UK*

Reaction of $[PtL][PF_6]_2$ (L = [12]aneS$_4$ = 1,4,7,10-tetrathiacyclododecane, [14]aneS$_4$ = 1,4,8,11-tetrathiacyclotetradecane or [16]aneS$_4$ = 1,5,9,13-tetrathiacyclohexadecane) with Cl_2–CCl_4 or Br_2–CCl_4 in MeCN solution afforded the corresponding platinum(IV) species $[PtX_2L][PF_6]_2$ in high yield as yellow (X = Cl) or orange (X = Br) solids. These species have been characterised by IR spectroscopy, FAB mass spectrometry and microanalytical data. Platinum-195 NMR spectroscopic studies on the parent platinum(II) complexes and on the platinum(IV) oxidation products confirm S_4 and S_4X_2 donor sets respectively. These studies also indicate that $[PtX_2([16]aneS_4)][PF_6]_2$ probably exist as *trans*-dihalides, whereas $[PtX_2([12]aneS_4)][PF_6]_2$ and $[PtX_2([14]aneS_4)][PF_6]_2$ are probably *cis*-dihalides. The crystal structure of $[Pt([16]aneS_4)][PF_6]_2 \cdot 2MeCN$ shows the Pt^{II} occupying a crystallographic inversion centre, co-ordinated to a square-planar tetrathia donor set with the free S-based lone pairs adopting the up, up, down, down configuration, Pt–S 2.310(2) Å. Platinum L-III edge EXAFS (extended X-ray absorption fine structure) data have been recorded for these complexes. The Pt–S bond lengths for the platinum(II) complexes compare well with those derived from single-crystal X-ray crystallography, while the Pt–S and Pt–X distances determined from EXAFS studies for the platinum(IV) complexes show that oxidation of Pt^{II} to Pt^{IV} typically results in a slight lengthening of the Pt–S bond lengths.

Platinum(IV) chemistry is largely dominated by complexes incorporating hard σ-donor or σ-donor/π-donor ligands such as amines and halides.[1] Examples of platinum(IV) species involving softer ligands such as phosphines, arsines, thioethers or selenoethers are less common, and the complexes are usually neutral with the general formula $[PtX_4(L\text{–}L)]$ (X = Cl or Br; L–L = bidentate Group 15 or 16 ligand).[1–3] Abel *et al.*[4,5] have reported the syntheses of several platinum(IV) thioether macrocyclic complexes based on the $[PtMe_3]^+$ fragment. We have previously reported the preparation of $[Pt([9]aneS_3)_2]^{4+}$ ([9]aneS$_3$ = 1,4,7-trithiacyclononane), $[Pt([18]aneS_6)]^{4+}$ ([18]aneS$_6$ = 1,4,7,10,13,16-hexathiacyclooctadecane) and $[Pt(Me_2[18]aneN_2S_4)]^{4+}$ (Me_2[18]aneN$_2$S$_4$ = 7,16-dimethyl-1,4,10,13-tetrathia-7,16-diazacyclooctadecane), the only other platinum(IV) thioether macrocyclic species known to date.[6–8] These species were generated from the parent platinum(II) complexes *via* electrochemical or chemical oxidation in strongly acidic media, and characterised *in situ* since they show only limited stabilities in solution and the solid state.

In this paper we report the reaction of $[PtL][PF_6]_2$ with X_2–CCl_4 (X = Cl or Br) to yield the stable cationic platinum(IV) complexes $[PtX_2L][PF_6]_2$ {L = 1,4,7,10-tetrathiacyclododecane([12]aneS$_4$), 1,4,8,11-tetrathiacyclotetradecane ([14]aneS$_4$) or 1,5,9,13-tetrathiacyclohexadecane ([16]aneS$_4$)}. Platinum-195 NMR spectroscopic and Pt L-III edge EXAFS (extended X-ray absorption fine structure) studies on both the platinum-(II) and -(IV) complexes are included, together with a single-crystal X-ray determination on the platinum(II) species $[Pt([16]aneS_4)][PF_6]_2 \cdot 2MeCN$.

Results and Discussion

The platinum(II) complexes $[PtL][PF_6]_2$ (L = [12]-, [14]- or [16]-aneS$_4$) were prepared as described previously.[9] Crystals of $[Pt([16]aneS_4)][PF_6]_2 \cdot 2MeCN$ were obtained by diffusion of Et_2O vapour into a solution of the complex in MeCN. The crystal structure shows the platinum(II) ion occupying a crystallographic inversion centre and co-ordinated to a precisely planar array of the four thioether donor atoms of the ligand, Pt–S(1) 2.310(2) and Pt–S(5) 2.310(2) Å, with the remaining, non-co-ordinated S-based lone pairs adopting an up, up, down, down configuration (Fig. 1, Table 1). This is the

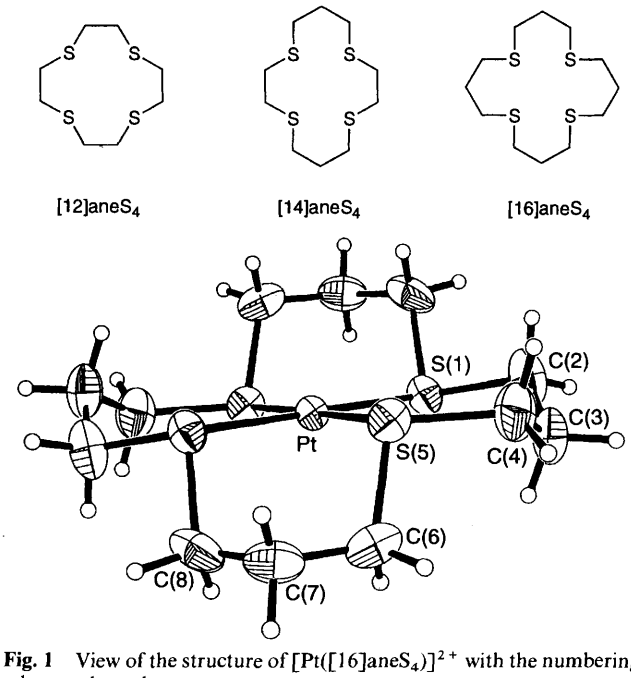

Fig. 1 View of the structure of $[Pt([16]aneS_4)]^{2+}$ with the numbering scheme adopted

Table 1 Selected bond lengths (Å) and angles (°) for complex **1**

Pt–S(5)	2.310(2)	C(4)–S(5)	1.802(8)
Pt–S(1)	2.310(2)	S(5)–C(6)	1.819(8)
S(1)–C(2)	1.813(8)	C(6)–C(7)	1.488(11)
C(2)–C(3)	1.461(11)	C(7)–C(8)	1.515(12)
C(3)–C(4)	1.463(11)	C(8)–S(1^{I})	1.810(8)
S(5)–Pt–S(1)	98.91(6)	C(4)–S(5)–C(6)	99.0(4)
C(8^{I})–S(1)–C(2)	102.2(4)	C(4)–S(5)–Pt	113.7(3)
C(8^{I})–S(1)–Pt	103.0(3)	C(6)–S(5)–Pt	105.5(3)
C(2)–S(1)–Pt	114.4(3)	C(7)–C(6)–S(5)	112.9(5)
C(3)–C(2)–S(1)	119.6(5)	C(6)–C(7)–C(8)	115.5(7)
C(2)–C(3)–C(4)	118.1(8)	C(7)–C(8)–S(1^{I})	109.6(5)
C(3)–C(4)–S(5)	114.8(6)		

Symmetry transformation used to generate equivalent atoms: I $-x+1, -y, -z+1$.

same ligand configuration as observed for the tetraselenoether analogue $[Pt([16]aneSe_4)]^{2+}$ [10] and contrasts with the structures of $[Pt([12]aneS_4)]^{2+}$ [Pt–S 2.266(4), 2.297(4) Å] [9,11] and $[Pt([14]aneS_4)]^{2+}$ [Pt–S 2.271(3), 2.285(4), 2.301(3), 2.295(4) Å],[12] both of which show an up, up, up, up configuration for the S-donor free lone pairs, with the platinum(II) ion displaced out of the least-squares S_4 plane by 0.28 Å in the former. The Pt–S bond lengths in $[Pt([16]aneS_4)]^{2+}$ are slightly longer than in the 12- and 14-membered ring analogues. A similar trend has been observed for *cis*-$[RhCl_2([14]aneS_4)]^{+}$ [Rh–S (*trans* to S) 2.3275(12) Å] and *trans*-$[RhCl_2([16]aneS_4)]^{+}$ [Rh–S 2.348(3) Å].[13] Also, structural studies on the series $[Pd([12]aneS_4)]^{2+}$ [Pd–S 2.280(4), 2.307(4) Å], $[Pd([14]aneS_4)]^{2+}$ [Pd–S 2.253(10)–2.296(8) Å] and $[Pd([16]aneS_4)]^{2+}$ [Pd–S 2.300(10)–2.315(9) Å] show that the palladium(II) ion is displaced out of the least-squares S_4 plane by 0.32 and 0.03 Å for the [12]- and [14]-aneS$_4$ complexes respectively, while it lies precisely within the plane of the macrocycle in the [16]aneS$_4$ species.[14] This illustrates that the hole size for [16]aneS$_4$ is a better match for the Pd^{II} than those of [12]- or [14]-aneS$_4$.

Addition of a solution of the appropriate halogen in CCl_4 to the colourless platinum(II) complexes $[PtL][PF_6]_2$ (L = [12]-, [14]- or [16]-aneS$_4$) in MeCN resulted in the formation of the yellow complexes $[PtCl_2L][PF_6]_2$ or the orange species $[PtBr_2L][PF_6]_2$. The FAB mass spectra revealed characteristic fragment ions in each case, consistent with the formulations presented above. The IR spectra provided clear evidence for both the macrocyclic ligand and PF_6^- anion in each case, and in certain cases weak Pt–X stretching vibrations could be tentatively assigned in the 200–400 cm^{-1} region, suggesting *cis*-dihalide arrangements for $[PtX_2([12]aneS_4)][PF_6]_2$ and $[PtX_2([14]aneS_4)][PF_6]_2$, and *trans*-dihalide arrangements for $[PtX_2([16]aneS_4)][PF_6]_2$.

^{195}Pt NMR spectroscopic studies

The ^{195}Pt NMR spectra were recorded for the platinum(II) parent species as well as the platinum(IV) products and the data are presented in Table 2. In each case, no other platinum-containing species were observed between δ −1500 and −5500. Each of the platinum(II) complexes $[PtL][PF_6]_2$ (L = [12]-, [14]- or [16]-aneS$_4$) exhibits a single resonance, with that for $[Pt([16]aneS_4)][PF_6]_2$ (δ −4177) occurring some 500 ppm downfield of those for the corresponding complexes involving the 12- and 14-membered macrocycles (δ −4690 and −4645 respectively). This may reflect the different configurations adopted by the 12- and 14-membered ring complexes (up, up, up, up) compared to that of the 16-membered ring system (up, up, down, down).[9,11,12] The ^{195}Pt NMR shifts for these platinum(II) tetrathioether species are downfield of those observed for platinum(II) species involving P_4 donor sets, *e.g.* $[Pt(Ph_2PCH_2CH_2PPh_2)_2]Cl_2$ (δ −5294) and $[Pt(Me_2PCH_2CH_2PMe_2)_2]Cl_2$ (δ −5312) (both quintets).[2] The ^{195}Pt NMR spectrum of the phosphathia macrocyclic species $[Pt(Ph_2[14]aneP_2S_2)]^{2+}$ ($Ph_2[14]aneP_2S_2$ = 8,12-diphenyl-1,5-dithia-8,12-diphosphacyclotetradecane) exhibits a triplet at δ −5174,[15] while the chemical shift for $[Pt([16]aneSe_4)]^{2+}$ ([16]aneSe$_4$ = 1,5,9,13-tetraselenacyclohexadecane) is very similar to those of the tetrathia complexes reported here, indicating a similar electronic environment at platinum for these Group 16 homologues.[10] For the platinum(II) dithioether complexes $[PtX_2\{MeS(CH_2)_nSMe\}]$ (n = 2 or 3), which involve S_2X_2 donor sets, the ^{195}Pt NMR shifts occur significantly downfield of those of the tetrathioether complexes described here.[2]

Table 2 ^{195}Pt NMR spectroscopic data[a]

Complex	δ(^{195}Pt)	Ref.
$[PtCl_2\{MeS(CH_2)_2SMe\}]$[b]	−3763, −3777	2
$[PtBr_2\{MeS(CH_2)_2SMe\}]$[b]	−4125, −4139	2
$[PtCl_2\{MeS(CH_2)_3SMe\}]$[b]	−3538, −3570	2
$[PtBr_2\{MeS(CH_2)_3SMe\}]$[b]	−3893, −3922	2
$[Pt([12]aneS_4)][PF_6]_2$	−4690	This work
$[Pt([14]aneS_4)][PF_6]_2$	−4645	This work
$[Pt([16]aneS_4)][PF_6]_2$	−4177	This work
$[Pt([16]aneSe_4)][PF_6]_2$	−4750[c]	10
$[Pt(Ph_2[14]aneP_2S_2)][PF_6]_2$	−5174[d]	15
$[PtCl_4\{MeS(CH_2)_2SMe\}]$[b]	−1899, −1910	2
$[PtBr_4\{MeS(CH_2)_2SMe\}]$[b]	−3053, −3065	2
$[PtCl_4\{MeS(CH_2)_3SMe\}]$[b]	−1630, −1649	2
$[PtBr_4\{MeS(CH_2)_3SMe\}]$[b]	−2760, −2779	2
cis-$[PtCl_2([12]aneS_4)][PF_6]_2$	−3417	This work
cis-$[PtBr_2([12]aneS_4)][PF_6]_2$	−3975	This work
cis-$[PtCl_2([14]aneS_4)][PF_6]_2$	−3313	This work
cis-$[PtBr_2([14]aneS_4)][PF_6]_2$	−3990	This work
trans-$[PtCl_2([16]aneS_4)][PF_6]_2$	−2587	This work
trans-$[PtBr_2([16]aneS_4)][PF_6]_2$	−3245	This work
trans-$[PtCl_2([16]aneSe_4)][PF_6]_2$	−3079	16
trans-$[PtBr_2([16]aneSe_4)][PF_6]_2$	−3785	16

[a] Spectra were recorded at 300 K in MeCN–CD_3CN, and the ^{195}Pt chemical shifts are relative to external 1 mol dm^{-3} $Na_2[PtCl_6]$ in water (δ 0). [b] Mixture of *meso* and DL isomers. [c] Spectrum recorded at 210 K in Me_2CO–$(CD_3)_2CO$. [d] Triplet.

In each case halogen oxidation to the corresponding platinum(IV) complexes $[PtX_2L]^{2+}$ results in a substantial downfield shift compared to the platinum(II) analogues. These oxidation shifts [*i.e.* $\delta(Pt^{IV}) - \delta(Pt^{II})$] are in the range 1200–1600 ppm for the dichlorides and 650–900 for the dibromides. The platinum(IV) complexes each show a single sharp resonance {$[PtX_2([12]aneS_4)]^{2+}$: X = Cl, δ −3417; Br, δ −3975. $[PtX_2([14]aneS_4)]^{2+}$: X = Cl, δ −3313; Br, δ −3990. $[PtX_2([16]aneS_4)]^{2+}$: X = Cl, δ −2587; Br, δ −3245} indicative of a single isomer in solution, and, importantly, the ^{195}Pt NMR chemical shifts are substantially upfield of those observed for $[PtX_4(MeSCH_2CH_2SMe)]$ or $[PtX_4(MeSCH_2CH_2CH_2SMe)]$.[2] Thus the data in Table 2 confirm that for these complexes there is a progressive shift to low frequency upon replacement of halide ligands by thioether sulfur donors, and between chloride and bromide ligands ($[PtCl_6]^{2-}$, δ 0). The values observed for $[PtX_2L][PF_6]_2$ (L = [12]-, [14]- or [16]-aneS$_4$) are therefore further strong evidence for their formulation as platinum(IV) complexes with S_4X_2 donor sets.

Similar behaviour was observed in the ^{195}Pt NMR spectra of the platinum(IV) selenoether macrocyclic complexes $[PtX_2([16]aneSe_4)][PF_6]_2$, and a single-crystal structure analysis of $[PtCl_2([16]aneSe_4)][PF_6]_2$ established beyond doubt the Se_4Cl_2 donor set at Pt^{IV} in that case.[16] Given that these selenoether species adopt a *trans*-dihalide arrangement with the platinum(IV) ion occupying the 16-membered

Table 3 Platinum L_{III}-edge EXAFS structural data[a]

Complex	d(Pt–S)[b]/Å	$2\sigma^2$[c]/Å^2	d(Pt–X)[b]/Å	$2\sigma^2$[c]/Å^2	R[d]	Fit index[e]
$[Pt([12]aneS_4)][PF_6]_2$	2.282(2)	0.0036(2)	—	—	22.9	3.4
$[Pt([16]aneS_4)][PF_6]_2$	2.315(2)	0.0051(3)	—	—	25.0	5.1
cis-$[PtCl_2([12]aneS_4)][PF_6]_2$	2.315(9)	0.0088(15)	2.329(9)	0.0032(9)	24.1	3.1
cis-$[PtBr_2([12]aneS_4)][PF_6]_2$	2.323(3)	0.0031(3)	2.486(2)	0.0031(3)	20.2	2.3
cis-$[PtCl_2([14]aneS_4)][PF_6]_2$	2.321(8)	0.0049(3)	2.347(3)	0.0020(4)	27.1	3.7
cis-$[PtBr_2([14]aneS_4)][PF_6]_2$	2.283(3)	0.0056(3)	2.465(15)	0.0274(30)	22.0	4.1
trans-$[PtCl_2([16]aneS_4)][PF_6]_2$	2.386(6)	0.0035(12)	2.287(12)	0.0043(19)	26.8	5.4
trans-$[PtBr_2([16]aneS_4)][PF_6]_2$	2.368(5)	0.0014(4)	2.449(6)	0.0070(18)	26.8	5.6

[a] Recorded in transmission mode on station 7.1 or 9.2, using powdered samples diluted with BN. [b] Standard deviations in parentheses. Note that the systematic errors in bond distances arising from data collection and analysis procedures are ±0.02–0.03 Å for well defined co-ordination shells. [c] Debye–Waller factor. [d] Defined as $(\int(\chi^T - \chi^E)k^3dk/\int\chi^E k^3dk) \times 100\%$. [e] Defined as $\Sigma i[(\chi^T - \chi^E)k_i^3]^2$.

macrocyclic cavity, it is highly likely that the thioether analogues $[PtX_2([16]aneS_4)][PF_6]_2$ also adopt a *trans*-dihalide geometry. This assignment is supported by the fact that $[RhCl_2([16]aneS_4)]PF_6$ also occurs as the *trans*-dichloride isomer;[13] since the ionic radius of Rh^{III} is larger than that for Pt^{IV}, on the basis of hole-size arguments a *trans* arrangement would also be expected for $[PtX_2([16]aneS_4)]^{2+}$.

In contrast, crystal structure analyses on $[MCl_2([14]aneS_4)]^{n+}$ (M = Rh,[13] Ir[17] or Cr,[18] n = 1; M = Ru,[19] n = 0) have revealed the *cis*-dihalide form in each case, with the tetradentate macrocycle adopting a folded arrangement. Given the restricted cavity size available, it is likely that *cis*-dihalide arrangements will also occur for $[PtX_2([12]aneS_4)][PF_6]_2$ and $[PtX_2([14]aneS_4)][PF_6]_2$. It is also worth noting that the oxidation shifts [*i.e.* $\delta(Pt^{IV}) - \delta(Pt^{II})$] for the thioether complexes are rather smaller for the 12- and 14-membered rings compared to those for the 16-membered ring, *i.e.* the platinum(IV) species $[PtX_2([16]aneS_4)]^{2+}$ occur significantly downfield of the corresponding 12- and 14-membered ring analogues. It has been shown previously that for the platinum(II) species $[PtCl_2L_2]$, L = PR_3 or AsR_3, the ^{195}Pt NMR shifts for the *cis* isomers occur 400 to 500 ppm upfield of the *trans* isomers.[20,21] In the absence of X-ray crystallographic data on the platinum(IV) complexes prepared in this work we cannot be absolutely certain of their geometries; however it is clear that they do involve S_4X_2 donor sets, and we suggest that the $[16]aneS_4$ complexes adopt *trans*-dihalide geometries, whereas the [12]- and [14]-$aneS_4$ complexes are probably *cis*-dihalide species.

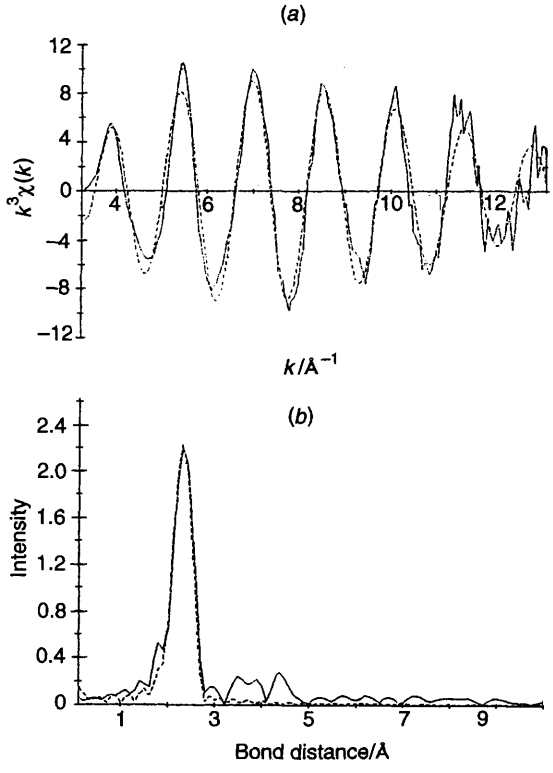

Fig. 2 Background-subtracted platinum L_{III}-edge EXAFS data (*a*) and the corresponding Fourier transform (*b*) for $[PtCl_2([16]aneS_4)][PF_6]_2$ (solid line = experimental, dashed line = calculated data)

Platinum L-III edge EXAFS structural studies

Several attempts were made to obtain crystals suitable for an X-ray study on one or more of the platinum(IV) complexes synthesised in this work, but without success. However, given the unusual nature of the complexes, and the paucity of structural data on platinum(IV) complexes involving soft Group 16 donor ligands, we proposed that metal-edge EXAFS data might provide useful information regarding the metal–ligand bond lengths for the first co-ordination sphere, *i.e.* d(Pt–S) and d(Pt–X). Importantly, the ^{195}Pt NMR spectroscopic studies carried out in parallel provided key information concerning the donor sets involved in these products (S_4X_2 in each case). Details of the refined EXAFS data for both the platinum-(II) and -(IV) complexes are given in Table 3 and Fig. 2 shows a typical example. The Pt L-III edge EXAFS spectra were recorded for the platinum(II) complexes $[PtL][PF_6]_2$ (L = [12]- or [16]-$aneS_4$) initially, in order to compare the Pt–S distances derived from this method with the *average* values obtained from X-ray crystallographic studies (2.282 and 2.310 Å respectively).[9,11,12] The EXAFS data were satisfactorily modelled to a first shell of four sulfurs giving Pt–S distances of 2.28 and 2.31 Å respectively. Thus, these results correlate closely with the X-ray data and confirm the potential of EXAFS studies for establishing bond lengths for the first co-ordination sphere in this particular class of compounds.

For the platinum(IV) species the EXAFS data were modelled for four sulfurs and two halogen atoms. No attempt was made to split the sulfur shell to take account of the slightly different distances expected for the Pt–S (*trans* to X) and Pt–S (*trans* to S) since X-ray structural studies on *cis*-$[MCl_2([14]aneS_4)]^+$ have shown that the difference is very small (*ca.* 0.02–0.04 Å) for M = Ir or Rh.[13,17]

Although strictly the absolute differences in d(Pt–S) are not significantly different for Pt^{II} *vs.* Pt^{IV} in some cases, certain trends are apparent. For *trans*-$[PtX_2([16]aneS_4)][PF_6]_2$ the EXAFS analyses reveal d(Pt–S) = 2.39 and 2.37 Å respectively for X = Cl and Br. Thus there is a slight lengthening of the Pt–S bond lengths upon oxidation of the platinum(II) species, consistent with the increase in co-ordination number from four to six. Similar behaviour was observed crystallographically for $[Pt([16]aneSe_4)]^{2+}$ [Pt–Se 2.420(3), 2.417(3) Å] *vs.* *trans*-$[PtCl_2([16]aneSe_4)]^{2+}$ [Pt–Se 2.4957(7), 2.5015(6); Pt–Cl 2.315(2) Å].[10,16] The crystal structure of *fac*-$[PtMe_3([9]aneS_3)]^+$ shows mean d(Pt–S) = 2.407 Å.[4] The

Pt–X distances for $[PtX_2([16]aneS_4)][PF_6]_2$ are 2.29 and 2.45 Å for X = Cl and Br respectively, with *d*(Pt–Cl) showing a good correlation with data for other platinum(IV) chlorides, *e.g.* *trans*-$[PtCl_2([16]aneSe_4)]^{2+}$ [Pt–Cl 2.315(2) Å] and *trans*-$[PtCl_2([14]aneN_4)]Cl{\cdot}HCl{\cdot}H_2O$ ([14]aneN$_4$ = 1,4,8,11-tetraazacyclotetradecane) [Pt–Cl 2.307(4) Å].[11]

For *cis*-$[PtX_2([12]aneS_4)][PF_6]_2$ and *cis*-$[PtX_2([14]aneS_4)][PF_6]_2$ the increase in *d*(Pt–S) upon oxidation of the platinum(II) species is smaller than for *trans*-$[PtX_2([16]aneS_4)][PF_6]_2$. This presumably reflects the *cis*-dihalide structures for the complexes with two S donors *trans* to X^-. Also, the greater *trans* influence of S over X^- leads to the observation that, for a given X, *d*(Pt–X) for the *cis* complexes are slightly longer than in *trans*-$[PtX_2([16]aneS_4)][PF_6]_2$, and *d*(Pt–S) *trans* to X are slightly shorter than *d*(Pt–S) *trans* to S. This effect will therefore partially counteract the lengthening expected upon increasing the co-ordination number from four (Pt^{II}) to six (Pt^{IV}).

Conclusion

The complexes $[PtX_2L][PF_6]_2$ (L = [12]-, [14]- or [16]-aneS$_4$) have been prepared in good yields and isolated as powdered solids. These are the first examples of platinum(IV) complexes derived from tetrathioether macrocyclic ligands. The ^{195}Pt NMR spectroscopic data provide strong evidence that each of these species involves an S_4X_2 donor set around the central Pt^{IV}, and suggest that the complexes $[PtX_2([16]aneS_4)][PF_6]_2$ are *trans* dihalides whereas $[PtX_2([12]aneS_4)][PF_6]_2$ and $[PtX_2([14]aneS_4)][PF_6]_2$ are probably *cis* dihalides. Platinum L-III edge EXAFS studies have provided data on the Pt–S and Pt–X bond lengths in these species. Typically there is a small lengthening of *d*(Pt–S) upon oxidation from Pt^{II} to Pt^{IV}. A crystal structure determination of $[Pt([16]aneS_4)][PF_6]_2{\cdot}2MeCN$ has established an up, up, down, down configuration for the sulfur lone pairs in the co-ordinated ligand.

Experimental

Infrared spectra were measured as KBr or CsI discs or as Nujol mulls using a Perkin-Elmer 983 spectrometer over the range 200–4000 cm^{-1}, solution UV/VIS spectra in quartz cells (1 cm path length) using a Perkin-Elmer Lambda19 spectrophotometer, mass spectra by electron impact (EI) or fast-atom bombardment (FAB) using 3-nitrobenzyl alcohol as matrix on a VG Analytical 70-250-SE normal-geometry double-focusing mass spectrometer. ^{195}Pt NMR spectra were recorded in 10 mm NMR tubes containing 10–15% deuteriated solvent using a Bruker AM360 spectrometer operating at 77.4 MHz and are referenced to 1 mol dm^{-3} aqueous $[PtCl_6]^{2-}$ [$\delta(^{195}Pt)$ 0]. Microanalyses were obtained from the Imperial College Microanalytical Laboratory. The complexes $[PtL][PF_6]_2$ (L = [12]-, [14]- or [16]-aneS$_4$) were prepared as described previously.[9] The EXAFS measurements were made at the Daresbury Synchrotron Radiation Source (SRS), operating at 2.0 GeV (*ca.* 3.2 × 10^{-10} J) with typical currents of 200 mA. Platinum L-III edge data were collected on station 7.1 using a silicon(111) order-sorting monochromator, or on station 9.2 using a double-crystal silicon(220) monochromator, with harmonic rejection achieved by stepping off the peak of the rocking curve by 50% of full height level. Data were collected in transmission mode from samples diluted with boron nitride and mounted between Sellotape in 1 mm aluminium holders.

Syntheses

$[PtCl_2([12]aneS_4)][PF_6]_2$. To a solution of $[Pt([12]aneS_4)][PF_6]_2$ (0.040 g, 0.055 mmol) in MeCN (5 cm^3) was added dropwise Cl_2–CCl_4 (2 cm^3) to give a yellow-orange solution. Addition of Et_2O afforded a yellow solid which was filtered off and dried *in vacuo* (yield = 0.035 g, 79%) (Found: C, 12.8; H, 2.3. $C_8H_{16}Cl_2F_{12}P_2PtS_4$ requires C, 12.7; H, 2.0%). FAB mass spectrum: *m*/*z* = 651, 580, 505, 471 and 434 {calc. for $[Pt^{35}Cl_2([12]aneS_4)(PF_6)]^+$ 648, $[Pt([12]aneS_4)(PF_6)]^+$ 580, $[Pt^{35}Cl_2([12]aneS_4)]^+$ 503, $[Pt^{35}Cl([12]aneS_4)]^+$ 468 and $[Pt([12]aneS_4)]^+$ 435}. IR spectrum (Nujol mull, CsI plates): 1155m, 835vs, 723w, 555m, *345w*, *320w** and 295w cm^{-1}.

$[PtBr_2([12]aneS_4)][PF_6]_2$. To a solution of $[Pt([12]aneS_4)][PF_6]_2$ (0.035 g, 0.048 mmol) in MeCN (5 cm^3) was added Br–CCl_4 (1 cm^3) to give an orange solution. Addition of Et_2O afforded a yellow-orange solid which was filtered off and dried *in vacuo* (yield = 0.037 g, 79%) (Found: C, 10.0; H, 1.9. $C_8H_{16}Br_2F_{12}P_2PtS_4{\cdot}CCl_4$ requires C, 10.4; H, 1.6%). FAB mass spectrum: *m*/*z* = 595, 580, 515 and 434 {calc. for $[Pt^{81}Br_2([12]aneS_4)]^+$ 595, $[Pt([12]aneS_4)(PF_6)]^+$ 580, $[Pt^{81}Br([12]aneS_4)]^+$ 514 and $[Pt([12]aneS_4)]^+$ 435}. IR spectrum (Nujol mull, CsI plates): 1300w, 1155w, 845s, 720w, 560m, 490w and 298 cm^{-1}.

$[PtCl_2([14]aneS_4)][PF_6]_2$. To a solution of $[Pt([14]aneS_4)][PF_6]_2$ (0.040 g, 0.054 mmol) in MeCN (5 cm^3) was added dropwise Cl_2–CCl_4 (2 cm^3) to give a yellow solution. Addition of Et_2O afforded a yellow solid (yield = 0.031 g, 70%) (Found: C, 14.6; H, 2.4. $C_{10}H_{20}Cl_2F_{12}P_2PtS_4$ requires C, 14.6; H, 2.5%). FAB mass spectrum: *m*/*z* = 607, 533, 499 and 462, {calc. for $[Pt([14]aneS_4)(PF_6)]^+$ 608, $[Pt^{35}Cl_2([14]aneS_4)]^+$ 533, $[Pt^{35}Cl([14]aneS_4)]^+$ 498 and $[Pt([14]aneS_4)]^+$ 463}. IR spectrum (CsI disc): 3010s, 2960s, 1420m, 1280m, 1235w, 1045w, 1020w, 840vs, 740w, 670vw, 560s, 490w, *370w* and *341w* cm^{-1}.

$[PtBr_2([14]aneS_4)][PF_6]_2$. To a solution of $[Pt([14]aneS_4)][PF_6]_2$ (0.030 g, 0.040 mmol) in MeCN (5 cm^3) was added Br_2–CCl_4 (1 cm^3) to give an orange solution. Addition of Et_2O afforded a yellow solid (yield = 0.037 g, 79%) (Found: C, 13.5; H, 2.3. $C_{10}H_{20}Br_2F_{12}P_2PtS_4$ requires C, 13.2; H, 2.2%). FAB mass spectrum: *m*/*z* = 769, 691, 624, 608 and 462 {calc. for $[Pt^{81}Br_2([14]aneS_4)(PF_6)]^+$ 770, $[Pt^{81}Br([14]aneS_4)(PF_6)]^+$ 689, $[Pt^{81}Br_2([14]aneS_4)]^+$ 625, $[Pt([14]aneS_4)(PF_6)]^+$ 608 and $[Pt([14]aneS_4)]^+$ 463}. IR spectrum (Nujol mull, CsI plates): 1090m, 830vs, 720m, 560s, 465m, *312w* and *292w* cm^{-1}.

$[PtCl_2([16]aneS_4)][PF_6]_2$. To a solution of $[Pt([16]aneS_4)][PF_6]_2$ (0.060 g, 0.077 mmol) in MeCN (5 cm^3) was added dropwise Cl_2–CCl_4 (2 cm^3) to give a yellow solution. Addition of Et_2O afforded a yellow solid (yield = 0.055 g, 84%) (Found: C, 17.0; H, 2.6. $C_{12}H_{20}Cl_2F_{12}P_2PtS_4$ requires C, 16.9; H, 2.80%). FAB mass spectrum: *m*/*z* = 636, 561, 527 and 491 {calc. for $[Pt([16]aneS_4)(PF_6)]^+$ 636, $[Pt^{35}Cl_2([16]aneS_4)]^+$ 561, $[Pt^{35}Cl([16]aneS_4)]^+$ 526 and $[Pt([16]aneS_4)]^+$ 491}. IR spectrum (Nujol mull, CsI plates): 1404m, 1322m, 1299m, 1247m, 1070w, 1023m, 905m, 878s, 846vs, 764s, 738m, 721s, 669w, 557s, 459w, *368m*, 325vw and 294vw cm^{-1}.

$[PtBr_2([16]aneS_4)][PF_6]_2$. To a solution of $[Pt([16]aneS_4)][PF_6]_2$ (0.060 g, 0.077 mmol) in MeCN (5 cm^3) was added Br_2–CCl_4 (1 cm^3) to give an orange solution. Addition of Et_2O afforded a yellow-orange solid (yield = 0.057 g, 79%) (Found: C, 15.1; H, 2.8. $C_{12}H_{24}Br_2F_{12}P_2PtS_4$ requires C, 15.3; H, 2.6%). FAB mass spectrum: *m*/*z* = 637, 571 and 491 {calc. for $[Pt([16]aneS_4)(PF_6)]^+$ 636, $[Pt^{81}Br([16]aneS_4)]^+$ 572 and $[Pt([16]aneS_4)]^+$ 491}. IR spectrum (Nujol mull, CsI plates): 1287m, 1198w, 1157w, 1017w, 967w, 877w, 839s, 763w, 721m, 557m and 294w cm^{-1}.

X-Ray crystallography

Colourless block-like crystals of $[Pt([16]aneS_4)][PF_6]_2{\cdot}2MeCN$ were obtained by diffusion of diethyl ether vapour into

* Italicised values are tentatively assigned to ν(Pt–X).

a solution of the complex in MeCN. The selected crystal (0.54 × 0.35 × 0.31 mm) was mounted on a glass fibre.

Crystal data. $C_{12}H_{24}F_{12}P_2PtS_4 \cdot 2CH_3CN$, $M = 863.69$, monoclinic, space group $P2_1/c$, $a = 11.1028(18)$, $b = 10.0998(15)$, $c = 13.1271(19)$ Å, $\beta = 100.15(2)°$, $U = 1449.0$ Å^3 [from 2θ values of 34 reflections measured at ±ω ($30 \leqslant 2\theta \leqslant 35°$, $\lambda = 0.710\,73$ Å)], $Z = 2$, $D_c = 1.980$ g cm^{-3}, $T = 293$ K, $\mu = 5.329$ mm^{-1}, $F(000) = 840$.

Data collection and processing. Stoe Stadi4 four-circle diffractometer, using graphite-monochromated Mo-Kα X-radiation, ω–2θ scans using the learnt-profile method.[22] 1890 Unique data collected ($2\theta_{max}$ 45°, h −11 to 11, k 0–10, l 0–14) of which 1532 had $F \geqslant 4\sigma(F)$ and 1877 were used in all calculations. No significant crystal decay or movement was observed.

Structure solution and refinement. The structure was solved by heavy-atom methods[23] which located the Pt atom on a crystallographic inversion centre. Iterative cycles of full-matrix least-squares refinement (on F^2) and Fourier-difference syntheses located all other non-H atoms in the half $[Pt([16]aneS_4)]^{2+}$ cation and one PF_6^- anion in a general position in the asymmetric unit.[24] During refinement two MeCN solvent molecules were also identified as associated with each $[Pt([16]aneS_4)]^{2+}$ cation. All non-H atoms were refined anisotropically, while H atoms were placed in fixed, calculated positions. The weighting scheme $w^{-1} = [\sigma^2(F_o^2) + (0.036P)^2 + 2.87P$ where $P = 1/3[\max(F_o^2, 0) + 2F_c^2]$ gave satisfactory agreement analyses. At final convergence R_1 $[F \geqslant 4\sigma(F)] = 0.0256$, wR_2 (all data) = 0.0630, S $(F^2) = 1.094$ for 171 refined parameters. The final ΔF synthesis showed no peaks above 0.54 e Å^{-3} and in the final cycle $(\Delta/\sigma)_{max}$ was 0.006.

Atomic coordinates, thermal parameters and bond lengths and angles, have been deposited at the Cambridge Crystallographic Data Centre (CCDC). See Instructions for Authors, *J. Chem. Soc., Dalton Trans.*, 1996, Issue 1. Any request to the CCDC for this material should quote the full literature citation and the reference number 186/92.

EXAFS Refinements

Typically two data sets were collected for each complex and the analyses were carried out on the averaged spectra. The raw data were background-subtracted using the program PAXAS[25] by fitting a six- or eight-order split polynomial to the pre-edge subtracted spectrum between $k = 2$ and 14–16 Å^{-1}. Curve fitting was carried out using the program EXCURVE 92.[26] Ground-state potentials of the atoms were calculated using Von Barth theory and phase shifts using Hedin–Lundqvist potentials. For the platinum(II) complexes one shell (4 × S) was fitted, while for the platinum(IV) systems two shells (4 × S and 2 × X, X = Cl or Br) were modelled. For the latter, EXAFS refinements were also carried out using S_6 or X_6, and in the case of X = Br the results clearly indicated S_4Br_2 donor sets. In the case of $[PtCl_2L][PF_6]_2$, the very similar back scattering from S and Cl made the assignment of the donor set difficult on the basis of the EXAFS data alone, however the ^{195}Pt NMR spectroscopic data provide very strong evidence for S_4Cl_2 donor sets and confirmed that no other Pt-containing species were present. The distances and Debye–Waller factors were refined for all the shells, as well as the Fermi energy difference. No attempt was made to refine the carbons of the ligand backbones since these occur over a range of distances and are not expected to be well defined.

Acknowledgements

We thank the EPSRC for support and Johnson Matthey plc for generous loans of $PtCl_2$. We also thank the Director of the SRS at Daresbury for the use of the facilities and we are indebted to Dr. W. Levason (University of Southampton) for help in collecting the EXAFS data.

References

1 See D. M. Roundhill, in *Comprehensive Coordination Chemistry*, eds. R. D. Gillard, J. A. McCleverty and G. A. Wilkinson, Pergamon, Oxford, 1987, vol. 5 and refs. therein.
2 E. G. Hope, W. Levason and N. A. Powell, *Inorg. Chim. Acta*, 1986, **115**, 187.
3 E. G. Hope, W. Levason, M. Webster and S. G. Murray, *J. Chem. Soc., Dalton Trans.*, 1986, 1003.
4 E. W. Abel, P. D. Beer, I. Moss, K. G. Orrell, V. Šik, P. A. Bates and M. B. Hursthouse, *J. Chem. Soc., Chem. Commun.*, 1987, 978.
5 E. W. Abel, P. D. Beer, I. Moss, K. G. Orrell, V. Šik, P. A. Bates and M. B. Hursthouse, *J. Organomet. Chem.*, 1988, **341**, 559.
6 A. J. Blake, R. O. Gould, A. J. Holder, T. I. Hyde, M. O. Odulate, A. J. Lavery and M. Schröder, *J. Chem. Soc., Chem. Commun.*, 1987, 118.
7 A. J. Blake, R. O. Gould, A. J. Lavery and M. Schröder, *Angew. Chem., Int. Ed. Engl.*, 1986, **25**, 274.
8 A. J. Blake, G. Reid and M. Schröder, *J. Chem. Soc., Dalton Trans.*, 1990, 3363.
9 A. J. Blake, A. J. Holder, G. Reid and M. Schröder, *J. Chem. Soc., Dalton Trans.*, 1994, 627.
10 N. R. Champness, P. F. Kelly, W. Levason, G. Reid, A. M. Z. Slawin and D. J. Williams, *Inorg. Chem.*, 1995, **34**, 651.
11 D. Waknine, M. J. Heeg, J. F. Endicott and L. A. Ochrymowycz, *Inorg. Chem.*, 1991, **30**, 3691.
12 M. A. Watzky, D. Waknine, M. J. Heeg, J. F. Endicott and L. A. Ochrymowycz, *Inorg. Chem.*, 1993, **32**, 4882.
13 A. J. Blake, G. Reid and M. Schröder, *J. Chem. Soc., Dalton Trans.*, 1989, 1675.
14 A. J. Blake and M. Schröder, *Adv. Inorg. Chem.*, 1990, **35**, 1.
15 N. R. Champness, C. S. Frampton, G. Reid and D. A. Tocher, *J. Chem. Soc., Dalton Trans.*, 1994, 3031.
16 W. Levason, J. J. Quirk, G. Reid and C. S. Frampton, *Inorg. Chem.*, 1994, **33**, 6120.
17 A. J. Blake, R. O. Gould, G. Reid and M. Schröder, *J. Organomet. Chem.*, 1988, **356**, 389.
18 N. R. Champness, C. S. Frampton, S. R. Jacob and G. Reid, *Inorg. Chem.*, 1995, **34**, 396.
19 T.-F. Lai and C.-K. Poon, *J. Chem. Soc., Dalton Trans.*, 1982, 1465.
20 A. Pidcock, R. E. Richards and L. M. Venanzi, *J. Chem. Soc. A*, 1968, 1970.
21 P. L. Goggin, R. J. Goodfellow, S. R. Haddock, B. F. Taylor and I. R. H. Marshall, *J. Chem. Soc., Dalton Trans.*, 1976, 459.
22 W. Clegg, *Acta Crystallogr., Sect. A*, 1981, **37**, 22.
23 G. M. Sheldrick, SHELX 86, *Acta Crystallogr., Sect. A*, 1990, **46**, 467.
24 G. M. Sheldrick, SHELXL 93, University of Göttingen, 1993.
25 N. Binsted, PAXAS, Program for the analysis of X-ray absorption spectra, University of Southampton, 1988.
26 N. Binsted, EXCURVE 92, SERC Daresbury Laboratory Program, 1992.

Received 29*th February* 1996; *Paper* 6/01451H